

Adsorptive optimization of green *Calotropis gigantea* silver nanoparticles: photocatalytic degradation against Congo red and Acid orange 7 dyes arbitrated by sunlight

M. Arslan^a, Raziya Nadeem^a, M. Idrees Jilani^{a,b}, Tariq Javed^{a,b}, Iram Javed^{b,*}

^aDepartment of Chemistry, University of Agriculture Faisalabad, Faisalabad, Punjab, Pakistan, Tel. +923186262212; email: arslanexpert07@gmail.com (M. Arslan), Tel. +923228669634; email: raziyaanalyst@yahoo.com (R. Nadeem)

^bDepartment of Chemistry, University of Sahiwal, Sahiwal, Punjab, Pakistan, Tel. +92 3039701075; email: iramjavedmughal07@gmail.com (I. Javed), Tel. +923320638261; email: idreeschemistry@gmail.com (M. Idrees Jilani), Tel. +92 3360916597; email: mtariq@uosahiwal.edu.pk (T. Javed)

Received 1 March 2021; Accepted 19 August 2021

ABSTRACT

A greener method was incorporated to synthesize nanoparticles of noble metal (Ag) from *Calotropis gigantea* silver nanoparticles (AgNPs) powdered leaf extract using silver nitrate (AgNO₃) solution. The fabricated silver NPs were characterized by X-ray diffraction and scanning electron microscopy. The observed average size of silver NPs assessed as 25–35 ± 0.17 nm with intraparticle distancing, possesses a cubic-spherical shape that is stable beyond 6 months without any accretion. The catalytic reduction of Congo red (CR) and Acid orange 7 (AO-7) dyes was observed with green *C. gigantea*-AgNPs arbitrated by sunlight as well as in absence of sunlight, respectively. Optimization of various parameters (pH, shaking time and dye concentration) was examined by UV-Vis spectrophotometer. *C. gigantea*-AgNPs catalytic degradation obeys pseudo-second-order kinetics together with a rate constant (K_2) in the presence and absence of sunlight and degradation is said to be physical sorption in nature. Isothermal data exhibit a trend of Freundlich > Temkin's > Langmuir with both dyes on the basis of regression (R^2) values. The percentage recyclability of *C. gigantea*-AgNPs gives their peak values in presence of sunlight: 96.11 with CR and 93.89 with AO-7, respectively.

Keywords: *Calotropis gigantea*-AgNPs; pH; Acid orange 7; Congo red; Sunlight; Percentage recyclability

1. Introduction

Nanotechnology has become an improved field concerned with research and innovations and deals with particles on a nanometer scale (1–100 nm). It is said to be capable of massively increasing production rate at a significantly reduced cost, which is one of the top priorities of the current era. Noble metallic NPs such as Ag (silver), Au (gold) and Pt (platinum), offer remarkable stability, simple chemical synthesis and tunable surface functionalization, which

have been more conveniently used in industrial products (such as pharmaceutical, cosmetics). The size of nanoparticles is acquired by the specifically controlled synthesis in order to get nanoparticles for a certain application. Among noble metal (Au, Ag, Pt) nanoparticles (NMNPs) have diverse areas of applications: in photodynamic therapy, skin diseases, biocidal-disinfectant, in catalysis and also possesses optical electro-dynamic properties in the development of chemical and biological sensors, respectively. In this framework, scientific research has evolved constantly,

* Corresponding author.

making it possible to explore newly synthesized materials and find their applications that may be cost-effective. In order to meet with high efficiency, less cost yield, green methods for NPs synthesis have become more approved procedures in recent days.

To develop green nanotechnology, naturally occurring materials such as plant extract, virus and bacteria are harmless that employ stable nanomaterials synthesis, respectively. In recent researches, plants are widely used to generate a variety of stable nanoparticles due to the presence of phytochemicals that are safest, less cost and give a high yield of biocompatible nanoparticles. Likewise, these phytochemicals: biomolecules, terpenoids, polysaccharides (proteins, vitamins) serve as both stabilizing and reducing agents themselves that require not much use of further stabilizing and reducing agents. Several plants such as *Aloe vera* [1], *Camellia japonica* [2], *Azadirachta indica* [3], *Cinnamomum* [4], *Gymnema sylvestre* [5] have effectively researched in the stable, bioactive and biocompatible synthesis of silver NPs that possesses potential applications in medicinal fields.

Synthetic organic dyes that form complexes in aqueous media evolve various environmental carcinogenic effects that develop toxicity towards neurogenic activities and affect reproductive organs are major discharge of industrial waste. Therefore, these synthetic dyes to be essentially removed from the aqueous environment. Adsorption has been extensively accounted for industrial processes rather than other purification techniques due to simplicity of design, less cost, the facile operating procedure for reduction of toxic substances from aqueous medium. Therefore, the removal of colorless and colored synthetic organic materials or toxicants from wastewater is regarded as the principal application of the adsorption process [12]. With respect to the current reported problem, photocatalysts: surface-modified TiO₂ NPs [29], Ag-NPs from polygonum [20], zinc sulfide nanoparticles [31] were studied as photocatalytic and hydrophobic properties of NPs with a breakdown of organic pollutants provides the chemical stability, efficient reductive, high reactivity and low-cost procedure. The photodegradation procedure brings down the intermediate activation energy (i.e., $\pi-\pi^*$ and $\sigma-\sigma^{**}$ excitation) and assists the reduction of organic pollutants from wastewater.

Calotropis gigantea (Giant calotrope) belongs to the family Apocynaceae and novel NPs have been reported from leaf extract of it [6]. The bark and root bark of *C. gigantea* used for medicine: for digestive disorders including stomach ulcer, in joint pain 7 for parasitic infections. Hence, *C. gigantea* is said to be an environmentally friendly plant that produces high-efficiency products [7,8]. In this work, Ag-NPs from *C. gigantea* leaf extract as a catalytic-adsorbent in the presence and absence of sunlight (visible light range 400–800 nm) were undertaken for adsorptive treatment of Acid orange 7 (AO-7) and Congo red (CR) dyes. Where *C. gigantea* surface modified by Ag-NPs proved to be a more effective surface for reduction of dyes from aqueous media, act as a catalyst. Among all the above reviews, there is a need to reveal an eco-friendly, high-efficiency desirable adsorption procedure by utilizing natural materials [10]. The present experimental studies are based on adsorption optimization of green *C. gigantea* silver nanoparticles (AgNPs) mediated by sunlight and in absence of sunlight for catalytic

degradation of two hazardous azo dyes: Congo red (CR) and Acid orange 7 (AO-7) from aqueous media [9].

2. Materials and methods

2.1. Chemicals

Silver nitrate (AgNO₃), sodium hydroxide (NaOH), sulphuric acid (H₂SO₄) and all other chemicals/reagents turned to account were of A. grade (analytical grade). Acid orange 7 and Congo red were obtained from Merck Pvt. Ltd., (Pakistan) and D-ionized water was put to use throughout the experiments [11].

2.2. *C. gigantea* leaf extract

C. gigantea leaves were collected from Botanical Garden, Department of Botany, University of Agriculture Faisalabad, Faisalabad, Pakistan. Leaves were purified systematically with D-ionized water to eliminate surface impurities and dried for 2 d at room temperature (288 ± 2 K). Then finely crushed powdered leaves biomass (10 g) was put to use with 200 mL D-ionized water, heated for 10 min and leave for 3 h [13]. By repeating the same procedure for a weak the extract was filtered, stored at -5°C and further utilized for the synthesis of silver nanoparticles.

2.3. Synthesis of *C. gigantea*-AgNPs

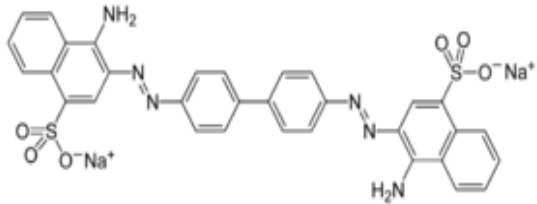
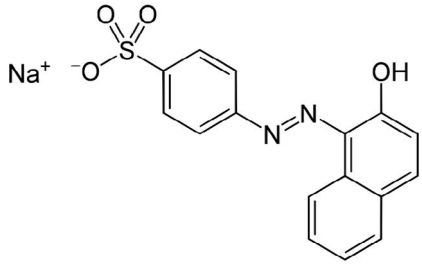
In a classical green synthetic procedure, 0.1 mol L⁻¹ solution of AgNO₃ was slowly added to freshly prepared *C. gigantea* leaf extract in 1:2 ratio and continuously stirred for 20 min. The color change from light brown to brown-yellow suggested that aqueous extract of *C. gigantea* generates highly stable silver NPs in D-ionized water. Similarly, biomolecules present in *C. gigantea* leaves biomass could behave as both reducing and stabilizing agents. The synthesized *C. gigantea*-AgNPs were stored at 277 K temperature that is stable beyond 6 months without any accrument and utilized for further catalytic experiments [1,31,32].

2.4. Catalytic degradation of Acid orange 7 and Congo red

Catalytic potential of green *C. gigantea*-AgNPs (0.1 g) was perceived for reduction of 1.0 mg L⁻¹ (stock) aqueous solution of Acid orange 7 (AO-7) and Congo red (CR) with the help of UV-Visible spectrophotometer at maximum absorption (λ_{max}) of 486 and 497 nm, respectively. In the absence of sunlight, CR stock gives 2.251 absorbances that is reduced to 2.249 in sunlight while, for AO-7 1.981 is reduced to 1.976 at their λ_{max} . Physio-chemical characters of dyes are presented in Table 1. With the help of different adsorption parameters (pH, contact time and dye concentration) in the presence and absence of sunlight, it was clearly observed that the color of corresponding dyes (AO-7 and CR) cautiously decreased and then bring to a colorless aqueous solution (100 mL), respectively.

In each degradation medium, the volume of AO-7 and CR solution was 100 mL, thoroughly mixed with 0.1 g desired adsorbent amount. Samples were examined at the variable contact time, pH and initial dye dosage and then filtered with 0.45 μ m PTFE-filter to get extract dye solution [32].

Table 1
Chemical and physical specifications of CR and AO-7

Primary name (abbreviation)	Congo red (CR)	Acid orange 7 (AO-7)
Chemical name	Sodium salt of 3,3'-([1,1'-biphenyl]-4,4'-diyl)-bis-(4-aminophthalene-1-sulphonic acid)	Monosodium salt of 4-[2-hydroxy-1-naphthyl]azo]benzenesulfonic acid
EC/CAS number	EC: 209-358-4 CAS: 573-58-0	EC: 211-199-0 CAS: 633-96-5
Empirical formula	$C_{32}H_{22}N_6Na_2O_6S_2$	$C_{16}H_{11}N_2NaSO_4$
Structural formula		
Physical form	Red brown powder, soluble in hot water	Orange powder soluble in water
Molecular weight	696.665 g mol ⁻¹	350.32 g mol ⁻¹
pKa	4.1 in water at 298 K	3.47 in water at 298 K
M.P	>360°C	164°C
Maximum absorbance (λ_{max})	497 nm	486 nm
Biological applications	Staining for gram -ve bacteria, for amyloidosis and for amyloid fibrils	In cosmetics: wound dressing materials

2.5. Percentage degradation efficiency

The percentage degradation of AO-7 and CR via *C. gigantea*-AgNPs catalyst in presence and absence of sunlight was calculated as:

$$\% \text{ degradation} = \frac{C_0 - C_e}{C_0} \times 100 \quad (1)$$

where C_0 (mg L⁻¹) and C_e (mg L⁻¹) are the concentration of dye before and after adsorption in solution. Experimental data were statistically analyzed on the average basis by taking 3 concordant readings for each experiment to lessen random errors.

2.6. Morphological characterization of *C. gigantea*-AgNPs

Surface identification of green AgNPs mediated by *C. gigantea* leaves biomass was executed by scanning electron microscopy (SEM) (JEOL JSM-6380 LA, Japan). X-ray diffraction pattern (Bruker model-D8, Germany) of *C. gigantea*-NPs was accomplished by phase identification at the 2 θ range from 20°–80° [14]. The particle size of *C. gigantea*-AgNPs (green) was determined by the following formula:

$$d = \frac{K\lambda}{\beta \cos\theta} \quad (2)$$

where d shows the crystal size of Ag nanoparticles, β (radians) is the full-width size at half-length at maximum, λ

is X-ray wavelength, K is constant and theta (θ) denotes Bragg's diffraction angle, respectively. The UV-Visible spectrophotometric (288 to 480 nm) analysis of green *C. gigantea* Ag nanoparticles was carried out at two different solution concentrations (1,000 and 750 mg L⁻¹) presented in Fig. 1. Fig. 1 illustrates sharp absorbance peaks in the range (410–450 nm) for each concentration, confirmed the presence of silver nanoparticles in colloidal solution [15,16].

3. Results and discussions

3.1. X-ray diffraction analysis of *C. gigantea*-AgNPs

The X-ray diffraction (XRD) a pattern of green AgNPs mediated by *C. gigantea* is illustrated as Fig. 1 (Bruker model-D8, Germany). The purity and crystalline structural morphology of bio-synthesized *C. gigantea*-AgNPs at optimized conditions were obtained by XRD studies. Four comprehensive peaks that are appeared at 38.82°, 45.98°, 65.33° and 78.66° which communicates the face-centered cubic-spherical AgNPs and are given as crystallographic planes: 111, 200, 220 and 311, respectively [17,19] (Fig. 2). The sharp appearing peaks in the XRD graph represent the formation of high crystalline regions in green *C. gigantea*-AgNPs with respect to small crystalline regions that are predicted on the basis of length and width of XRD peaks. The main phase of XRD that appeared in the graph related to AgNPs are well accord with the standard diffraction pattern of joint committee (JCPDS) file no. (04-07830) [18]. The particle

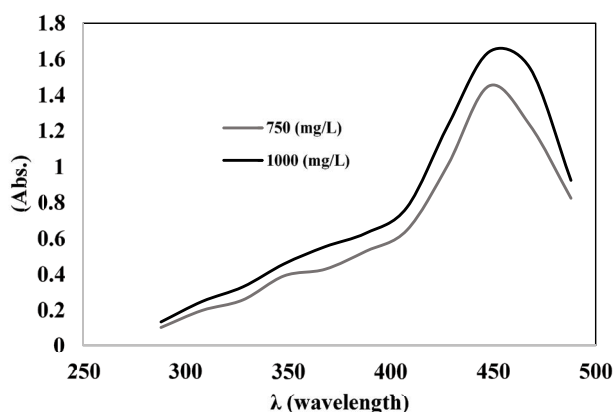


Fig. 1. UV-Visible studies of green *Calotropis gigantea*-AgNPs.

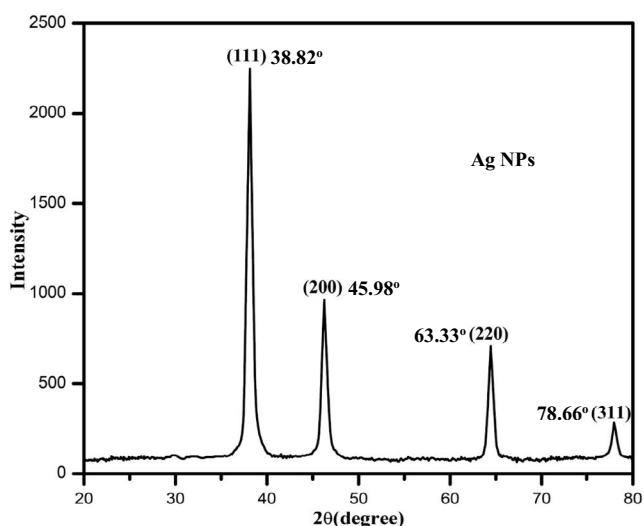


Fig. 2. XRD-graph of green Ag-NPs mediated by *Calotropis gigantea*.

size of green *C. gigantea*-AgNPs was further determined by Scherrer's equation:

$$d = \frac{K\lambda}{\beta \cos\theta} \quad (3)$$

$$\text{Theta } (\theta) = \frac{\pi}{180} \times \beta \quad (4)$$

where d represents the crystal size of Ag nanoparticles, β (radians) is the full-width size at half-length at maximum (FWHM), λ (1.45 Å) is X-ray wavelength, K is constant (0.9) and theta (θ) denotes Bragg's diffraction angle, respectively. The calculated average particle size of green *C. gigantea*-AgNPs was 25.11 in nanometers.

3.2. Morphological (SEM) analysis of *C. gigantea*-AgNPs

Scanning electron micrographs (SE-micrographs) empowered visualization of the size and shape of the green silver nanoparticles (Fig. 3). SEM-analysis of the green synthesized

C. gigantea-AgNPs clearly represents clusters and irregular shapes (trough regions), mostly aggregated in the form of lumps and having an average 20 to 35 nm (10–17 nm diameter) size with interparticle distance, which magnified two ($\times 20,000$ and $\times 40,000$) times (Figs. 3a and 4b) [20]. The rough morphology of the *C. gigantea*-AgNPs provides excellent photocatalytic activity for both corresponding synthetic dyes (AO-7 and CR). Additionally, the SEM images exhibit that the availability of a large surface area of NPs enhances the percentage degradation of AO-7 and CR from aqueous solution mediated by sunlight and in dark mode, respectively. Thus, SEM analysis showed the maximum estimated particle size between 25 to 110 nm as well as the cubic-spherical structure of the nanoparticles. Particle size was confirmed by the XRD pattern of nanostructures [21]. Fig. 3c and d show the agglomeration effect of dye molecules (CR and AO-7) on the adsorbent surface. Dye molecules facilitate pore filling towards the NPs surface and agglomeration gets increased.

3.3. Catalytic activity of *C. gigantea*-AgNPs

The catalytic potential (activity) of green synthesized NPs has been of consequential interest via various supporting parameters: pH, shaking time and dye concentration. In this study, *C. gigantea*-AgNPs as a nano-catalyst was investigated for percentage reduction of Acid orange 7 (AO-7) and Congo red (CR) dyes mediated by sunlight (medium-2) M_2 as well as in dark M_1 (medium-1) mode. The degradation efficiency was examined at room temperature 288 ± 2 K (in dark mode) and temperature fluctuations in presence of sunlight were measured by using a plastic digital-thermometer, respectively [23].

Effectiveness of pH on photocatalytic (M_2) and dark (M_1) reduction of AO-7 (pH 2–8) and CR (pH 4–10) was investigated by proceeding 100 mg L⁻¹ initial dye concentration, 0.1 g of *C. gigantea*-AgNPs catalyst with shaking time of 100 min at room temperature (288 ± 2 K) for dark and temperature fluctuation 288 ± 6 K was measured for adsorption solution mediated by sunlight. Fig. 4a and b represent the effect of pH on photo-catalytic and dark reduction of AO-7 and CR dye on AgNPs of *C. gigantea*, respectively. In batch reduction experiments, CR percentage degradation increased from 93 to 97.88 in dark and 94.43%–99.04% mediated by sunlight with pH rise from 4 to 8 [22,24]. While AO-7 percentage degradation increased from 91.27% to 96.12% in dark and in sunlight 92.9% to 98.16% with a rise in pH from 2 to 6. *C. gigantea*-AgNPs acquits differently in sunlight and in dark and maximum dye degradation was measured as 97.88% and 91.27% in dark for CR and AO-7 and 99.04% and 96.12% in sunlight for CR and AO-7. From Fig. 4a and b, no further dye reduction was observed with an increase in pH from 8–10 in the case of CR and 6–8 in the AO-7 adsorptive degradation medium. CR (azo dye) degradation becomes more advantageous due to the presence of charged amino group (protonated) at pH 8.0 and negatively charged *C. gigantea*-AgNPs surface provide an active area that dye molecules exhibit favorability in sunlight at high temperature as compared to in dark mode. Besides, at lower pH 6.0 AO-7 molecule gives its conjugated form that facilitates electrostatic pull b/w dye molecule and *C. gigantea*-AgNPs catalyst surface

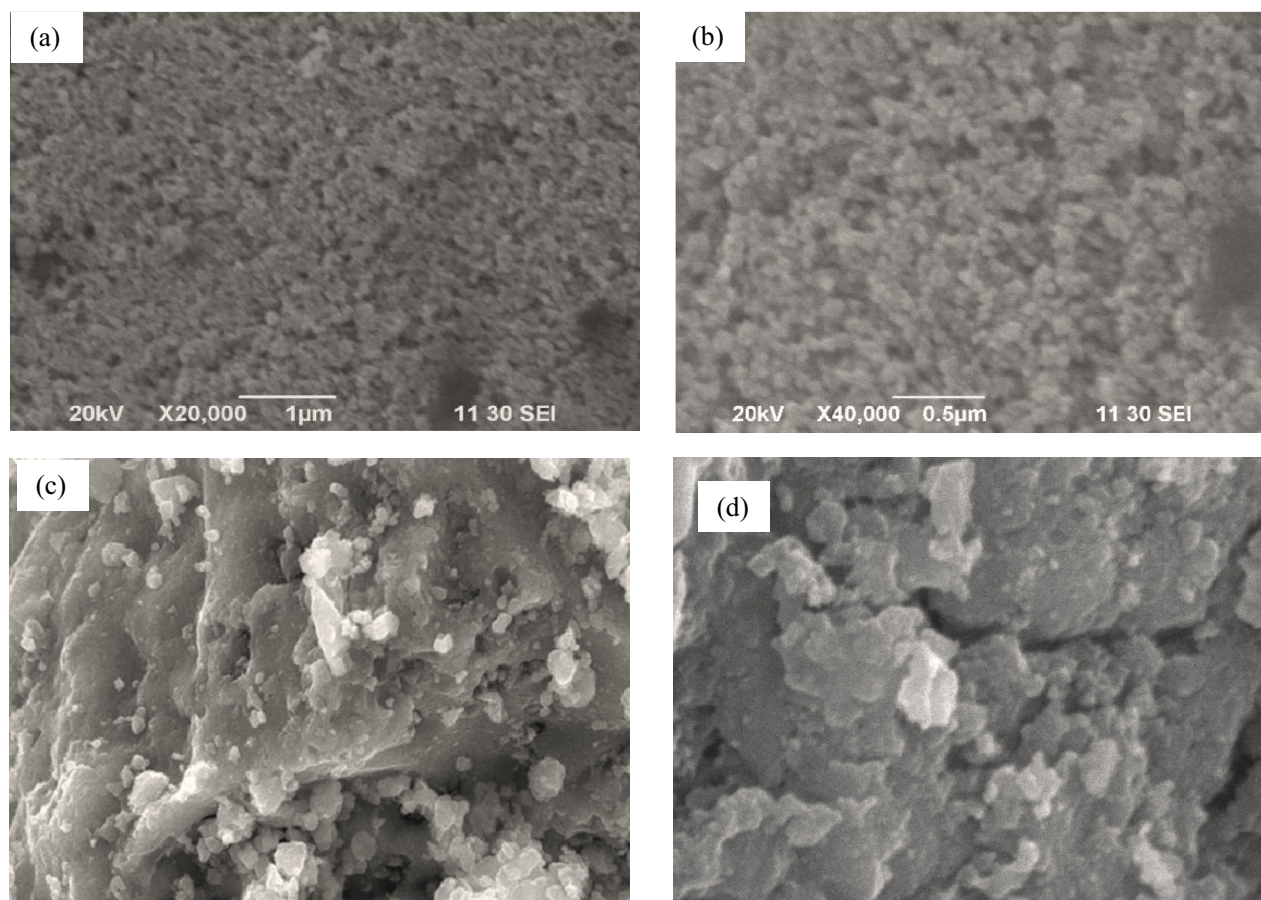


Fig. 3. Morphological representation of native (a) X 20,000, (b) X 40,000 and loaded (c) CR, (d) AO-7 of cubic-spherical *Calotropis gigantea*-AgNPs.

respectively. Therefore at 8.0 and 6.0 pH for CR and AO-7, dye molecules give rise to auspicious degradation, is chemisorption and said to be endothermic in nature [25].

The catalytic adsorptive reduction of AO-7 and CR as a parametric function of initial concentration (mg L^{-1}) of dyes was monitored from 10 to 150 mg L^{-1} . Other adsorption experimental variables were kept as 0.1 g adsorbent (*C. gigantea*-AgNPs) mass, pH 8.0 and 6.0 for CR and AO-7, 100 mL dye solution for both M_1 (293 ± 1 K) and M_2 (293 ± 4 K) with a contact time of 100 min, respectively. From Fig. 5a and b, it is entirely clear that dye degradation was decreased from 87% to 45.3% (M_1) and 90.4% to 57% (M_2) corresponds to CR (Fig. 5a). While, 95% to 55.6% (M_1) and 99.03% to 64.6% (M_2) corresponds to AO-7 dye with AgNPs as a catalyst, respectively (Fig. 5b). The behavior of percentage dye degradation may be attributed to a characteristic abundance of active sites at lower concentration are more conveniently available on *C. gigantea*-AgNPs surface. But, by increasing dye solution concentration the catalytic activity of NPs reduced due to the turgidity of adsorbent binding sites with respect to corresponding dye molecules.

To analyze the behavior of AgNPs arbitrated by *C. gigantea*, for catalytic reduction of CR and AO-7 as a function of shaking time (15–180 min) effect was determined

in the presence (M_2) and absence (M_1) of sunlight from aqueous media. Catalytic potential of *C. gigantea*-AgNPs was demonstrated via other optimum conditions with 0.1 g adsorbent mass, 75 mg L^{-1} (CR) and 100 mg L^{-1} (AO-7) dye concentration at optimized pH (8.0 for CR and 6.0 for AO-7) and almost identical behavior was perceived with the adsorbent surface for both dyes (Fig. 6a and b). The catalytic reduction potential increased from 89.66% to 96.1% (M_1) and 94.41% to 94.72% (M_2) for CR and 91.16% to 96.55% (M_1) and 91.48% to 99.47% (M_2) corresponds to Acid orange 7 with an increase in time duration from 15–180 min. The percentage degradation results investigate that *C. gigantea*-AgNPs proved to be a more efficient adsorbent for catalytic degradation of synthetic dyes (AO-7 and CR) arbitrated by sunlight. In addition, at starting point effective rise in percentage dye adsorption is possibly due to high surface pore-sites availability which is more accessible in medium-2 rather than medium-1 [27].

Moreover, as the time duration reached towards 90–180 min (AO-7), and 60 to 180 min (CR) the catalytic efficiency of green *C. gigantea*-AgNPs was decelerated and eventually get equilibrium phase resulting due to adsorbent sites saturation and may also due to less efficient forces grow between adsorbent (NPs) and dye molecules, respectively.

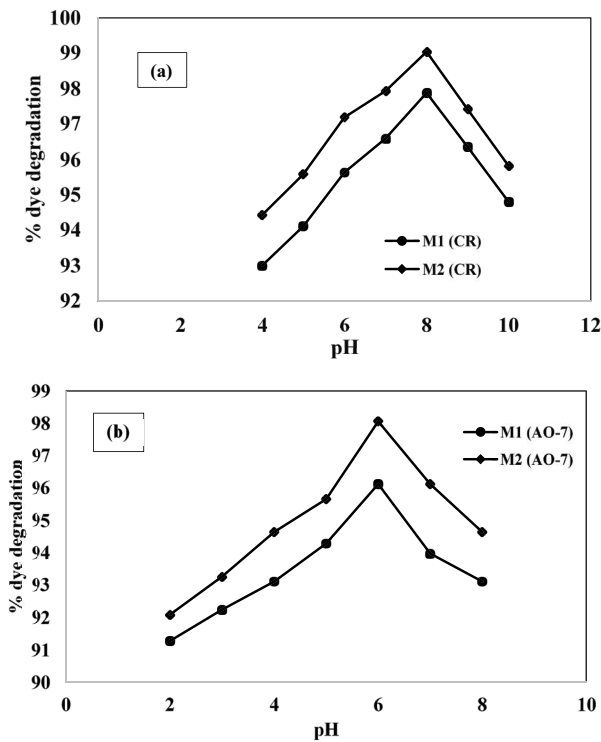


Fig. 4. pH effect on *Calotropis gigantea*-AgNPs in dark (M_1) and (a) arbitrated by sunlight (M_2) (b) for synthetic dyes.

3.4. Kinetics

Kinetic parameters gives information about effectiveness of catalytic adsorption of NPs and execute-ability of studied operations. On governing, the catalytic adsorption data with respect to contact time (15–180 min) was applied to the first-order Lagergren equation [5] and pseudo-second-order rate equation by utilizing the linearized forms:

$$\log(q_e - q_t) = \log q_e - \frac{K_1}{20,303} t \tag{5}$$

$$\frac{t}{q_t} = \frac{1}{K_2 q_e^2} + \frac{1}{q_e} t \tag{6}$$

where q_t and q_e are the concentrations of AO-7 and CR (mg g^{-1}) appearing at equilibrium corresponds to the time interval studied and K_1, K_2 represent equilibrium rate constants for pseudo-first and second-order kinetic catalytic-adsorption models. The above linearized representative expressions for both kinetic models are used in plotted graph forms of t/q_t vs. t and $\log(q_e - q_t)$ vs. t in Figs. 7a, b and 8a, b, their parameter values are enclosed in Table 2. Applicability comparison of both models was carried out on a regression equation basis.

3.5. Isothermal explanation

That equilibrium adsorption model based on a mono-layer (Langmuir) [28] mechanism on silver NPs mediated

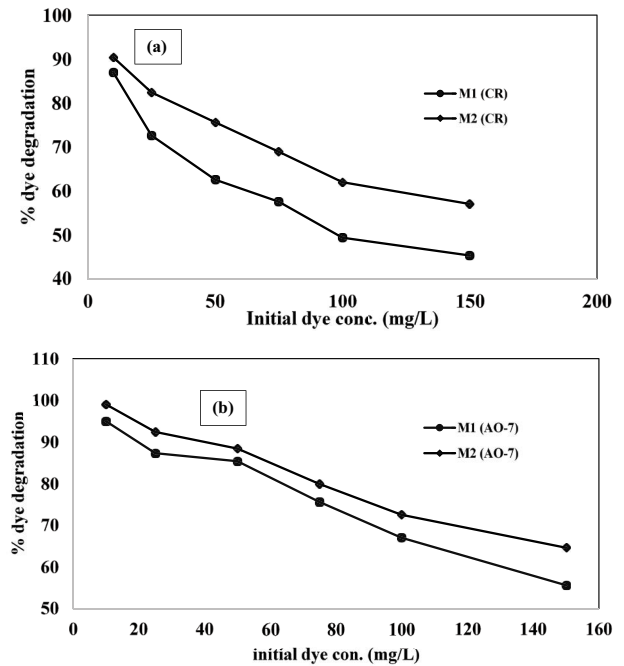


Fig. 5. Initial dye influence on *Calotropis gigantea*-AgNPs in dark (M_1) (a) and arbitrated by sunlight (M_2) (b) for synthetic dyes (0.1 g) *Calotropis gigantea*-AgNPs; 100 min contact time.

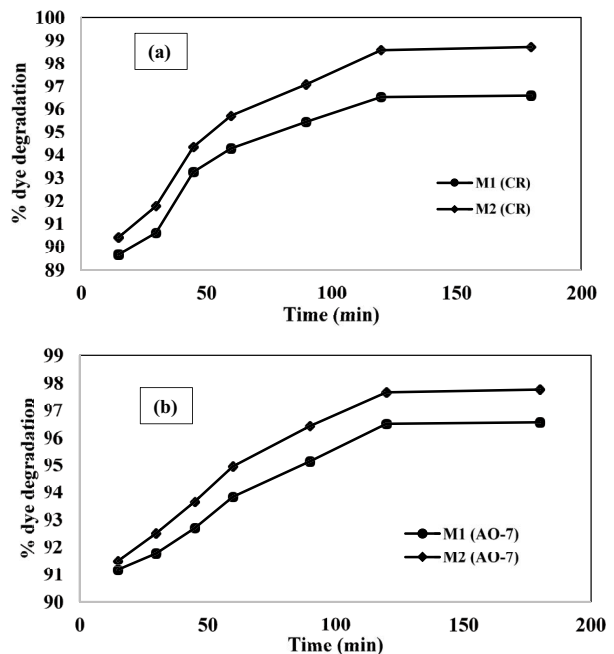


Fig. 6. Contact time influence on *Calotropis gigantea*-AgNPs in dark (M_1) (a) and sunlight (M_2) (b) for synthetic dyes reduction.

by *C. gigantea* surface with respect to synthetic dyes (AO-7 and CR), linearized as:

$$\frac{C_e}{C_{\text{ads}}} = \frac{1}{q_m} \times \frac{1}{K_L} + \frac{C_e}{q_m} \tag{7}$$

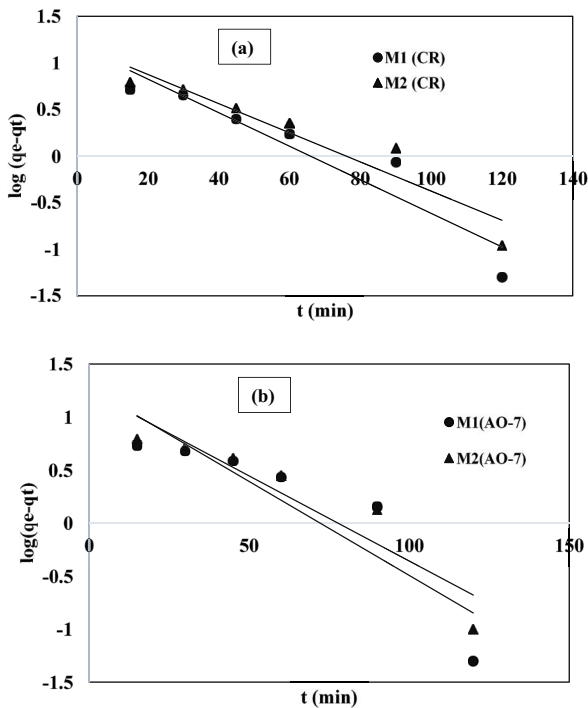


Fig. 7. Pseudo-first-order linear plot for synthetic dyes AO-7 (b) and CR (a) catalytic adsorption on green *Calotropis gigantea*-AgNPs.

where C_{ads} is the concentration of dye adsorbed on green *C. gigantea*-AgNPs surface at equilibrium (mg g^{-1}), C_e is the concentration of dye in the selective volume of solution (100 mL) at equilibrium (mg L^{-1}), q_m (mono-layer adsorption potential) of *C. gigantea*-AgNPs (mg g^{-1}) and K_L (Langmuir model constant) measured in L mg^{-1} . A linear plot was obtained C_e/C_{ads} vs. C_e (10–150 mg L^{-1}) as given in Fig. 9a and b which exhibits that the catalytic adsorption process is not monolayer and can be multilayer physisorption. In Table 3, according to calculated monolayer adsorption capacity values, the catalytic adsorption mediated by green *C. gigantea*-AgNPs is more dominating in presence of sunlight rather than in dark mode.

The heterogeneity of adsorbent (*C. gigantea*-AgNPs) surface (Freundlich) [29] towards AO-7 and CR adsorption was measured by linear mathematical isotherm representation as:

$$\log C_{ads} = \frac{1}{n} \log C_e + \log K_f \quad (8)$$

Table 2

Kinetic parameters for catalytic adsorption of AO-7 and CR dyes over green *Calotropis gigantea*-AgNPs

Kinetic models	Parameters	M ₁ (CR)	M ₂ (CR)	M ₁ (AO-7)	M ₂ (AO-7)
Pseudo-first-order	q_e (mg g^{-1})	0.171	0.174	0.245	0.221
	K_1	0.041	0.034	0.045	0.037
	R^2	0.891	0.901	0.808	0.873
Pseudo-second-order	q_e (mg g^{-1})	78.12	34.01	29.98	31.76
	K_2 (mg g^{-1})	7.1×10^{-3}	2.8×10^{-3}	5.4×10^{-3}	3.3×10^{-3}
	R^2	1	1	0.999	1

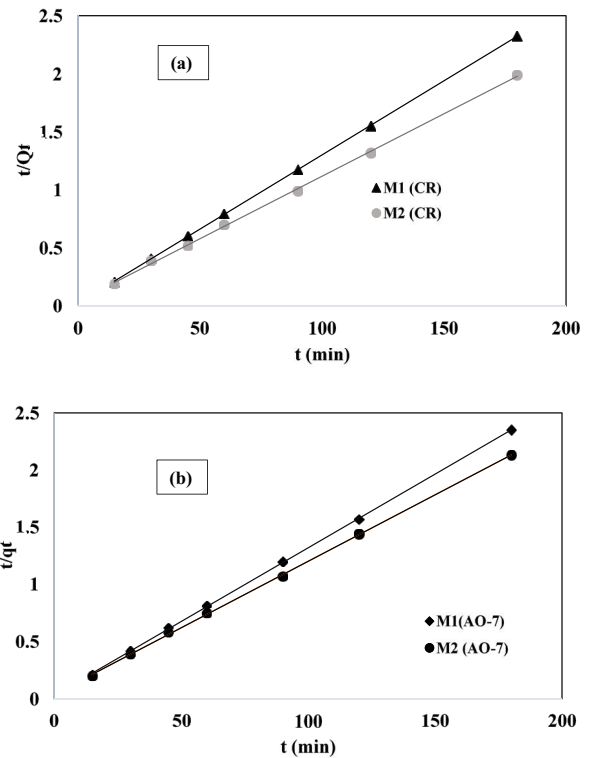


Fig. 8. Pseudo-second-order linear plot for synthetic dyes AO-7 (b) and CR (a) catalytic adsorption on green *Calotropis gigantea*-AgNPs.

where K_f ($\text{mg g}^{-1} \text{L}^{-1}$) is Freundlich catalytic-mechanism constant and n (intensity of adsorption) is NPs surface heterogeneity, C_{ads} is the AO-7 and CR concentration (mg g^{-1}) adsorbed on green *C. gigantea*-AgNPs surface at equilibrium phase, C_e is the concentration of corresponding dyes at equilibrium in solution (bulk). The numeric values of parameters are obtained from the slope (m) and intercept (c) by graphical plot between $\log C_{ads}$ vs. $\log C_e$ are presented in Fig. 10a and b, respectively. The R^2 values of Freundlich plot 0.996 (M_1) and 0.998 (M_2) with AO-7 and 0.995 (M_1) and 0.992 (M_2) with CR proposed that the catalytic-adsorption mechanism is heterogeneous on the basis of regression (linearity) values.

Similarly, linear representation of heat of adsorption measuring model (Temkin's) [30] that is resultant of NPs and dye-molecular interaction, expressed as:

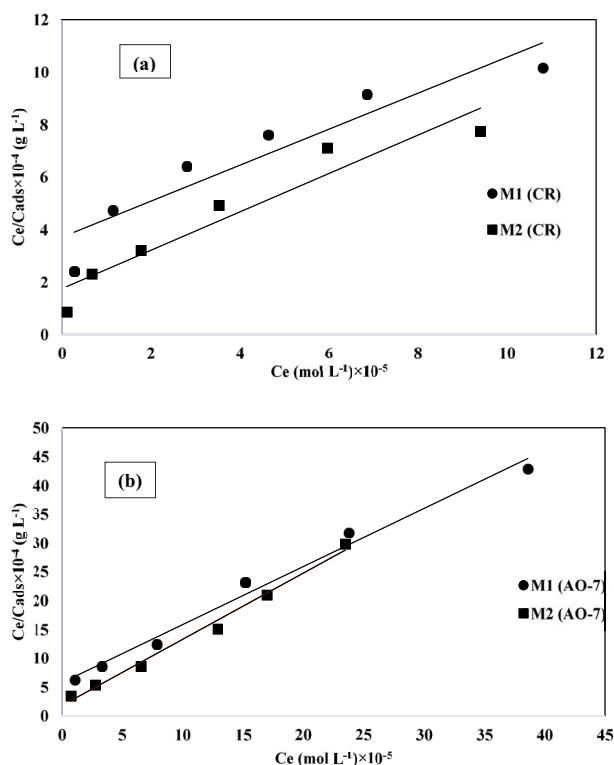


Fig. 9. Langmuir plot for synthetic dyes (AO-7 (b) and CR (a)) degradation by green *Calotropis gigantea*-AgNPs.

$$C_{\text{ads}} = B \ln A_T + B \ln C_e \quad (9)$$

where B is equal to RT/K_T (heat of adsorption) measured in (J mol^{-1}) , T in Kelvin is the measured temperature, R is the gas constant $(\text{J K}^{-1} \text{mol}^{-1})$, $1/K_T$ values (Table 3) indicates the catalytic-adsorption efficiency of green *C. gigantea*-AgNPs in mg L^{-1} , Parameter (A) is the maximum equilibrium binding energy constant in L mg^{-1} . The linear presented plot of C_{ads} vs. $\ln C_e$ (Fig. 11a and b) gives R^2 values (Table 3) that are slightly lower than Freundlich isotherm, is said to be an appropriate adsorption isotherm for experimental calculated data of synthetic dyes (AO-7 and CR) on AgNPs mediated by *C. gigantea*, respectively.

Table 3

Isotherm parameters for catalytic adsorption of AO-7 and CR dyes over green *Calotropis gigantea*-AgNPs

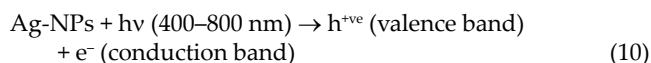
Adsorption isotherms	Parameters	M_1 (CR)	M_2 (CR)	M_1 (AO-7)	M_2 (AO-7)
Langmuir	q_m (mg g^{-1})	136.5	145.6	80.64	93.45
	K_L ($\text{dm}^3 \text{mol}^{-1}$)	1.85×10^{-5}	4.2×10^{-5}	2.15×10^{-5}	8.14×10^{-5}
	R^2	0.882	0.916	0.994	0.967
	n	1.64	2.03	2.33	2.51
Freundlich	K_f (mg g^{-1})	0.153	0.015	-0.355	-0.104
	R^2	0.995	0.992	0.996	0.998
	B (J mol^{-1})	2.148	0.332	0.274	0.357
Temkin's	K_T (L mol^{-1})	4.12×10^5	11.4×10^5	2.26×10^5	10.5×10^5
	R^2	0.956	0.978	0.973	0.978

4. Percentage reusability

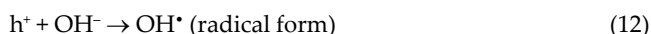
The percentage desorption inspection assists to elucidate the complexation of the adsorption mechanism and to recover the dyes (AO-7 and CR) from an aqueous solution using the corresponding adsorbent. Cyclic attempts were assembled to highlight effective percentage desorption of Acid orange 7 and Congo red by utilizing 0.5 N nitric acid (HNO_3) solution. Percentage desorption results of AO-7 and CR by green *C. gigantea*-AgNPs are shown in Table 4. It was perceived that the percentage of catalytic desorption synthetic dyes remains almost the same compared with percentage catalytic adsorption results. This suggests that by applying diluted solutions of 0.5 N nitric acid (HNO_3) for percentage desorption green *C. gigantea*-AgNPs serve as a good reusable adsorbent for recovery of AO-7 and CR dyes from an aqueous environment.

5. Mechanism

The photodegradation mechanism of dyes (AO-7 and CR) on the *C. gigantea*-AgNPs surface is complex due to the collusion of particular factors that effectuate adsorbent-adsorbate interactivity. The interactions may positive or negative and the bonding of dye-molecules with adsorbent-surface are determined by properties of the adsorbent surface, functional groups present in dyes. The designed mechanism was feasibly predicted on the basis of changes in morphological structure (SEM) of green synthesized Ag-NPs. The photoadsorption reduction of dyes can be predicted beyond band gap energies that facilitate the prompting of the conduction band (e^-) and valence bands (h^{+ve}) when sunlight falls on a photoadsorption medium [32].



Reduction degradation:



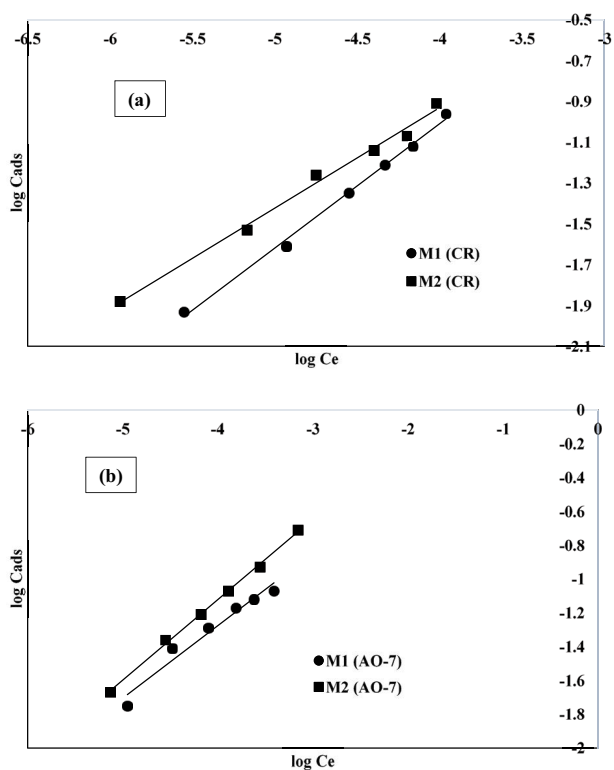
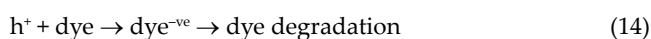


Fig. 10. Freundlich plot for synthetic dyes (AO-7 (b) and CR (a)) degradation by green *Calotropis gigantea*-AgNPs.

Oxidation:



In the above equations, the holes in h^+ (valence band) exist as an oxidizing agent, leads to the oxidative degradation of dyes while e^- (conduction band electrons) behave as a reducing agent that reduces adsorbent-surface oxygen, leads to the reductive adsorption of dyes (AO-7 and CR) from aqueous media.

Similarly, in dark reduction of dyes the pore sites of green synthesized *C. gigantea*-AgNPs are rapidly available but due to the unavailability of an external light source the mechanism of bandgap energies cannot proceed in a rapid form. Therefore, there is a less percentage of dye degradation in dark in comparison with sunlight, respectively.

Table 4
Percentage catalytic desorption of AO-7 and CR dyes over green *Calotropis gigantea*-AgNPs

No. of cycles	% desorption			
	D-M ₁ (CR)	D-M ₂ (CR)	D-M ₁ (AO-7)	D-M ₂ (AO-7)
1	95.23	87.50	78.46	93.89
2	96.11	89.70	80.29	91.64
3	94.96	82.45	77.75	88.27

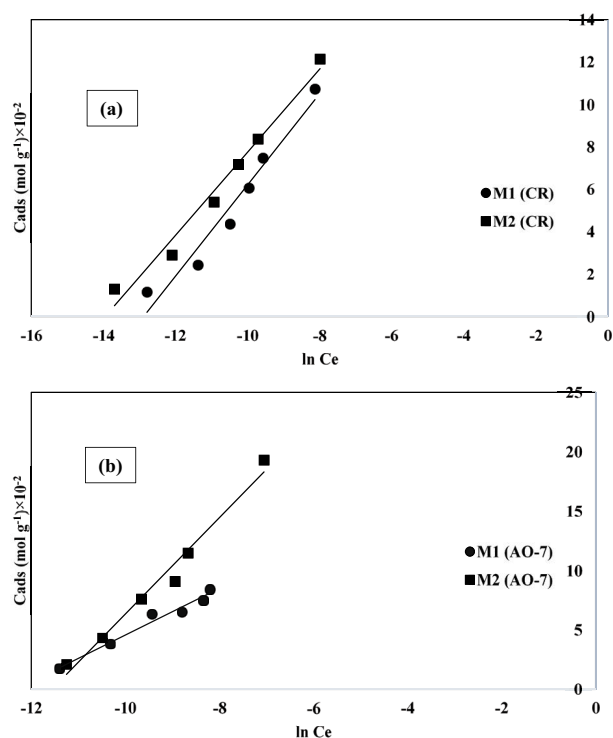


Fig. 11. Temkin isotherm plot for synthetic dyes (AO-7 (b) and CR (a)) degradation by green *Calotropis gigantea*-AgNPs.

6. Conclusion

Ag colloidal solutions have been rapidly synthesized in a green environment, chemically. In these proceedings, we have tested the catalytic activity of green synthesis of AgNPs mediated by *C. gigantea* in an aqueous solution in the presence and absence of sunlight without any reducing/stabilizing agents. The UV-Visible spectral graph represented that these green synthesized NPs samples possess absorbance peaks in the 410–450 nm range. The average measured size of *C. gigantea*-AgNPs is about 20–35 nm with an average diameter of 10–17 nm by SEM images. The calculated data are well depicted by Freundlich and Temkin’s isotherm recommended favorable adsorption isotherm for AO-7 and CR dyes on *C. gigantea*-AgNPs. The data relating to kinetic explanation indicated that the catalytic-adsorption kinetics of dyes on *C. gigantea*-AgNP obey the pseudo-second-order model. The regenerated catalytic-desorption efficiency of green

C. gigantea-AgNPs was found to be more effective in 0.5 N nitric acid solution. The present study results concluded that green *C. gigantea*-AgNPs is an efficient adsorbent for catalytic reduction of Acid orange 7 and Congo red in dark and arbitrated by sunlight.

References

- [1] S. Prathap Chandran, M. Chaudhary, R. Pasricha, A. Ahmad, M. Sastry, Synthesis of gold nanotriangles and silver nanoparticles using *Aloe vera* plant extract, *Biotechnol. Progr.*, 22 (2006) 577–583.
- [2] R. Karthik, M. Govindasamy, S.-M. Chen, Y.-H. Cheng, P. Muthukrishnan, S. Padmavathy, A. Elangovan, Biosynthesis of silver nanoparticles by using *Camellia japonica* leaf extract for the electrocatalytic reduction of nitrobenzene and photocatalytic degradation of Eosin-Y, *J. Photochem. Photobiol., B*, 170 (2017) 164–172.
- [3] S.S. Shankar, A. Rai, A. Ahmad, M.J. Sastry, Rapid synthesis of Au, Ag, and bimetallic Au core-Ag shell nanoparticles using neem (*Azadirachta indica*) leaf broth, *J. Colloid Interface Sci.*, 275 (2004) 496–502.
- [4] J. Huang, Q. Li, D. Sun, Y. Lu, Y. Su, X. Yang, H. Wang, Y. Wang, W. Shao, N. He, J. Hong, C. Chen, Biosynthesis of silver and gold nanoparticles by novel sundried *Cinnamomum camphora* leaf, *Nanotechnology*, 18 (2007) 105104–105114.
- [5] J. Reddy Nakkala, M. Rani, E. Bhagat, S.R. Sadras, Green synthesis of silver and gold nanoparticles from *Gymnema sylvestre* leaf extract: study of antioxidant and anticancer activities, *J. Nanopart. Res.*, 17 (2015) 151–176.
- [6] P. Ajith, A.S. Murali, H. Sreehari, B.S. Vinod, A. Anil, S.S. Chandran, Green synthesis of silver nanoparticles using *Calotropis gigantea* extract and its applications in antimicrobial and larvicidal activity, *Mater. Today: Proc.*, 18 (2019) 4987–4991.
- [7] L. Bulgariu, L.B. Escudero, O.S. Bello, M. Iqbal, J. Nisar, K.A. Adegoke, F. Alakhras, M. Kornaros, I. Anastopoulos, The utilization of leaf-based adsorbents for dyes removal: a review, *J. Mol. Liq.*, 276 (2019) 728–747.
- [8] S.S.R. Albeladi, M.A. Malik, S.A. Al-thabaiti, Facile biofabrication of silver nanoparticles using *Salvia officinalis* leaf extract and its catalytic activity towards Congo red dye degradation, *J. Mater. Res. Technol.*, 9 (2020) 10031–10044.
- [9] P. Singh, M. Halder, S. Ray, A. Bose, K. Sen, Green synthesis of silver and palladium nanocomposites: a study of catalytic activity towards etherification reaction, *Mater. Adv.*, 1 (2020) 2937–2952.
- [10] P. Balaji, B. Vignesh, M. Sowmiya, M. Meena, L. Lokesh, 2015, Removal of colour from textile effluent using natural adsorbent (*Calotropis gigantea*), *Int. J. Innovations Eng. Technol. (IJJET)*, 5 (2015) 265–272.
- [11] J. Sivakumar, C. Premkumar, P. Santhanam, N. Saraswathi, Biosynthesis of silver nanoparticles using *Calotropis gigantea* leaf, *Afr. J. Basic Appl. Sci.*, 3 (2011) 265–270.
- [12] B. Vaseeharan, C. Gunapoorani Sargunar, Y.C. Lin, J.C. Chen, Green synthesis of silver nanoparticles through *Calotropis gigantea* leaf extracts and evaluation of antibacterial activity against *Vibrio alginolyticus*, *Nanotechnol. Dev.*, 2 (2012) e3, doi: 10.4081/nd.2012.e3
- [13] A.A. Kamaru, N.S. Ahmad-Jani, N.A.N.N. Malek, N.S. Sani, Adsorptive removal of methylene blue and Acid orange 7 by hexadecyltrimethylammonium bromide modified rice husk, *J. Technol. (Sci. Eng.)*, 78 (2016) 7824, doi: 10.11113/jt.v78.7824.
- [14] C. Rajkuberan, K. Sudha, G. Sathishkumar, S. Sivaramakrishnan, Antibacterial and cytotoxic potential of silver nanoparticles synthesized using latex of *Calotropis gigantea* L., *Spectrochim. Acta, Part A*, 136 (2015) 924–930.
- [15] M.M. Khan, J. Lee, M.H. Cho, Au@TiO₂ nanocomposites for the catalytic degradation of methyl orange and methylene blue: an electron relay effect, *J. Ind. Eng. Chem.*, 20 (2014) 1584–1590.
- [16] R.F. Elsupikhe, K. Shamel, M.B. Ahmad, N.A. Ibrahim, N. Zainudin, Green sonochemical synthesis of silver nanoparticles at varying concentrations of κ-carrageenan, *Nanoscale Res. Lett.*, 10 (2015) 916, doi 10.1186/s11671-015-0916-1.
- [17] H.A. El-Adawy, A.A. Alomari, Evaluation of *Calotropis procera* fruits as a bioadsorbent for removing of Acid red 73 dye from the aqueous solutions, *Egypt. J. Chem.*, 63 (2020) 3217–3228.
- [18] P. Debnath, N.K. Mondal, 2020, Effective removal of Congo red dye from aqueous solution using biosynthesized zinc oxide nanoparticles, *Environ. Nanotechnol. Monit. Manage.*, 14 (2020) 100320, doi: 10.1016/j.enmm.2020.100320.
- [19] C. Vidya, H. Shilpa, M.N. Chandraprabhab, M.A. Lourdu Antonyraja, I.V. Gopala, A. Jaina, K. Bansal, Green synthesis of ZnO nanoparticles by *Calotropis gigantea*, *Int. J. Curr. Eng. Technol., Special Issue 1* (2013) 118–120.
- [20] N.N. Bonnia, M.S. Kamaruddin, M.H. Nawawi, S. Ratim, H.N. Azlina, E.S. Ali, Green biosynthesis of silver nanoparticles using 'Polygonum *Hydropiper*' and study its catalytic degradation of Methylene blue, *Procedia Chem.*, 19 (2016) 594–602.
- [21] S. Priya, K. Murugan, A. Priya, D. Dinesh, C. Panneerselvam, G. Durga Devi, B. Chandramohan, P. Mahesh Kumar, D.R. Barnard, R.-D. Xue, J.-S. Hwang, M. Nicoletti, R. Chandrasekar, A. Amsath, R. Bhagooli, H. Wei, Green synthesis of silver nanoparticles using *Calotropis gigantea* and their potential mosquito larvicidal property, *Int. J. Pure Appl. Zool.*, 2 (2014) 128–137.
- [22] S.M. Roopan, G. Elango Vijay, D. Devi Priya, I.V. Asharani, B. Kishore, S. Vinayprabhakar, N. Pragatheshwaran, K. Mohanraj, R. Harshpriya, S. Shanavas, R. Acevedo, Sunlight mediated photocatalytic degradation of organic pollutants by statistical optimization of green synthesized NiO NPs as catalyst, *J. Mol. Liq.*, 293 (2019) 111509, doi: 10.1016/j.molliq.2019.111509.
- [23] J. Pal, M.K. Deb, D.K. Deshmukh, D. Verma, Removal of methyl orange by activated carbon modified by silver nanoparticles, *Appl. Water Sci.*, 3 (2013) 367–374.
- [24] T. Varadavenkatesan, R. Selvaraj, R. Vinayagam, 2016, Phytosynthesis of silver nanoparticles from *Mussaenda erythrophylla* leaf extract and their application in catalytic degradation of methyl orange dye, *J. Mol. Liq.*, 221 (2016) 1063–1070.
- [25] M. Saeed, M. Siddique, M. Ibrahim, N. Akram, M. Usman, M.A. Aleem, A. Baig, *Calotropis gigantea* leaves assisted biosynthesis of ZnO and Ag@ZnO catalysts for degradation of rhodamine B dye in aqueous medium, *Environ. Prog. Sustainable Energy*, 39 (2020) e13408, doi: 10.1002/ep.13408.
- [26] B. Hu, S.-B. Wang, K. Wang, M. Zhang, S.-H. Yu, Microwave-assisted rapid facile "green" synthesis of uniform silver nanoparticles: self-assembly into multilayered films and their optical properties, *J. Phys. Chem. C*, 112 (2008) 11169–11174.
- [27] T.T. Bhosale, H.M. Shinde, N.L. Gavade, S.R. Babar, V.V. Gawade, S.R. Sabale, R.J. Kamble, B.S. Shirke, K.M. Garadka, Biosynthesis of SnO₂ nanoparticles by aqueous leaf extract of *Calotropis gigantea* for photocatalytic applications, *J. Mater. Sci.: Mater. Electron.*, 29 (2018), doi: 10.1007/s10854-018-8669-0.
- [28] C. Umamaheswari, A. Lakshmanan, N.S. Nagarajan, Green synthesis, characterization and catalytic degradation studies of gold nanoparticles against Congo red and Methyl orange, *J. Photochem. Photobiol., B*, 178 (2018) 33–39.
- [29] A. Mohammadi, K.A. Aliakbarzadeh, Methylene blue removal using surface-modified TiO₂ nanoparticles: a comparative study on adsorption and photocatalytic degradation, *J. Water Environ. Nanotechnol.*, 2 (2017) 118–128.
- [30] M. Ghaedi, A. Ansari, F. Bahari, A.M. Ghaedi, A. Vafaei, A hybrid artificial neural network and particle swarm optimization for prediction of removal of hazardous dye brilliant green from aqueous solution using zinc sulfide nanoparticle loaded on activated carbon, *Spectrochim. Acta, Part A*, 137 (2015) 1004–1015.
- [31] M. Zulfikar, R. Nadeem, T. Javed, M.I. Jilani, I. Javed, Green synthesis of Fe nanoparticles by using *Mangifera indica* extract and its application in photo-catalytic degradation of dyes, *Water Sci. Technol.*, 83 (2021) 1739–1752.